Available online at www.sciencedirect.com
SCIENCE DIRECT®
Fusion Engineering and Design 72 (2004) 149–168
Fusion Engineering and Design
www.elsevier.com/locate/fusengdes

Ignited spherical tokamaks and plasma regimes with LiWalls

L.E. Zakharov[a,*], N.N. Gorelenkov[a], R.B. White[a], S.I. Krasheninnikov[b], G.V. Pereverzev[c]

[a] *Princeton Plasma Physics Laboratory, MS-27, P.O. Box 451, Princeton, NJ 08543-0451, USA*
[b] *University of California, San Diego, Energy Research Center, La Jolla, CA 92093, USA*
[c] *Max-Plank-Institute für Plasmaphysik, D-85748 Garching bei München, Germany*

Available online 13 October 2004

Abstract

Basic requirements of the fusion power reactor and its development are outlined. The notion of operational power reactor regime (OPRR) is introduced explicitly for the first time in order to distinguish it from the relatively short ignition phase of the reactor operation. Development of OPRR is intrinsically linked to two basic technology objectives, i.e., development of the first wall (FW) and the tritium cycle (TC). The paper reveals an existing fundamental gap in the reactor development path associated with the lack of necessary amounts of tritium for the reactor design development. In this regard, low recycling regimes with a plasma limited by a lithium wall surface suggest enhanced stability and energy confinement, both necessary for tokamak power reactors. These regimes also could make ignition and OPRR feasible in compact tokamaks. Ignited spherical tokamaks (IST), self-sufficient in the bootstrap current, are introduced as a necessary interim step for development OPRR-FW-TC for the power reactors.

PACS: 28.52-s; 28.52.Av; 28.52.Cx; 52.55.Fa; 52.55.-s; 52.55.Tn

Keywords: Tokamaks; Fusion reactor; Ignition; First wall; Tritium; DD fusion

1. Introduction

At present, tokamak research is entering a new phase when the fusion produced α-particle heating will dominate over the external input of energy into the plasma [1]. Still there will be, at least, two more phases on the road to a reactor after this "burning", sub-critical plasma development. They include demonstration of ignition, and development of the regime and associated technology for power production.

Burning and ignition can be achieved and demonstrated with essentially conventional plasma regimes. An enhancement of size, magnetic field (together with the cost of the machine) are required. Although not yet envisioned, a short ignited phase, probably, can be achieved in the next generation of toka-maks, like ITER, with a modest improvement of confinement.

On the other hand, power production needs a special regime, called here an operational power reactor regime, or OPRR. OPRR requires 4–5 times higher power density than ignition and needs a plasma with significantly enhanced stability and confinement properties.

* Corresponding author. Tel.: +1 609 243 2630; fax: +1 609 243 2662.
E-mail address: lzakharov@pppl.gov (L.E. Zakharov).

0920-3796/$ – see front matter © 2004 Elsevier B.V. All rights reserved.
doi:10.1016/j.fusengdes.2004.07.015

The conventional tokamak regimes have a peaked plasma temperature as their most prominent characteristic. With high recycling at the plasma edge, and apparently producing plasma edge consistent with the material surfaces, this feature, at the same time, leads to substantial consequences limiting the tokamak core performance: turbulent energy losses [2], degradation of confinement with the power [3], Troyon limitations of plasma beta [4,5], possibility of sawtooth relaxations and internal collapse [6], instabilities at high edge density [7], etc.

The second characteristics is that a conventional plasma is separated from the stabilizing wall surface by a "vacuum" gap, and, thus, is prone to free boundary MHD instabilities, which further reduce the stability margins. As a result, stability, confinement degrading with the power, and overall performance remain insufficient for a power reactor.

This paper emphasizes that the search for new plasma regimes in tokamaks is unavoidable for development of a magnetic fusion reactor. Enhancement in stability and confinement are two of the requirements.

A fusion reactor requires a certain level of plasma pressure (0.8–1 MPa) for power production. For magnetic fields $B \simeq 5$ T such a pressure corresponds to beta values of 8–10 %. For aspect ratios $R/a > 3$ (determined by shielding from neutrons and radiation) conventional regimes with peaked plasma temperature are limited by much lower stability margins, e.g., $\beta = 2.7\%$ in ITER, probably, $\beta \simeq 4\%$ in future, which are too small for a power reactor.

Hypothetically, at higher magnetic fields, e.g., $B \simeq$ 7.5 T, the conventional regimes can approach the reactor plasma pressure even with moderate $\beta \simeq 4\%$. The problem is (besides numerous technological issues) that the experimental data base for stability margins at high fields will remain absent until fusion power will be used at full extent for the plasma heating. Also, fast degradation of the energy confinement τ_E with the heating power P, i.e. $\tau \propto P^{-\alpha P}$, $\alpha_P > 0.5$ in conventional plasma precludes reaching OPRR af-ter plasmas have been ignited.

The second reason is limited availability of tritium. The development of the first wall (or FW, considered here as the first 10–15 cm of material structure faced by fusion neutrons) would require consumption of a large amount of tritium (about 1 kg/m^2 for accumulating the neutron fluence of 15 MW-year/m^2). *Only compact, spherical tokamaks (ST) are suitable for this purpose*. Even though relatively small, these devices still should be self-sufficient in tritium and breed it with 100% efficiency or even more. Moreover, in order to use the entire wall surface for breeding *ignition is a necessary condition* to allow filling all NBI ports with a tritium breeding material after ignition has been reached.

A possible candidate for a mission of FW development could be an ignited spherical tokamak (IST), discussed further in this paper. The high beta ($\beta > 40\%$ and 35% achieved already) compensates a relatively small magnetic field, only possible for ST. At the same time, the problem of non-inductive current drive should be solved for ST. Conventional plasma regimes cannot provide sufficient confinement, fusion power density and bootstrap current for an IST. Thus, with the conventional plasma there is a gap on the development path to a reactor (even with use of high magnetic fields or low aspect ratio).

The alternative could be a low recycling plasma with high edge temperature, which would correspond to another class of confinement and stability regimes. Good plasma pumping by a lithium surface opens the possibility for a high temperature pedestal. If combined with core fueling, it creates a new confinement regime, where energy losses are determined by the particle diffusion, rather than by thermo-conduction. In contrast to thermo-conduction, diffusion is ambipolar and, thus, the losses are determined by the best confined plasma species. As a result, better confinement is expected in the low recycling regime.

At the same time, a lithium surface allows for a conducting (back up) wall situated right at the plasma boundary, thus, potentially eliminating free boundary instabilities. This would be a crucial improvement allowing not only approaching the OPRR stability requirement, but also leading to smaller and less costly experiments.

It is shown in this paper that with high edge temperature, the ignition and stationary regimes in ST seem to be possible. ISTs could be unique devices for developing the physics and technology of the power reactor.

Section 2 of the paper summarizes the basic requirements of the reactor development and motivation for new plasma regimes. Section 3 discusses the basic transport properties of the LiWall regime. Section 4

outlines the particle and energy extraction capabilities of LiWalls. Section 5 explains the stability enhancement for LiWall limited plasma. Section 6 discusses IST stabilty, self-sufficiency of bootstrap current, and stabilization of micro-turbulence.

2. Basic physics and technology aspects of the fusion reactor

Among numerous issues there are three specific objectives of magnetic fusion which should be developed for the fusion reactor

(1) Ignition and operational power reactor regime (OPRR).
(2) Design of the low activation first wall (FW) together with power extraction and helium ash exhaust.
(3) Tritium cycle (TC).

When existing plasma physics results together with technology and economic aspects are taken into account, the development of the fusion reactor appears to be rather restricted by fundamental constraints. Thus, a clear distinction should be drawn between the ignition phase (with low plasma beta and high energy confinement) and continuous OPRR (with high beta and reduced energy confinement). In its turn, the very development of OPRR requires use of fusion power for reaching the necessary plasma parameters and for stability limit studies.

Use of fusion power is extremely restricted by limitations on tritium consumption (besides many other technology and safety aspects). As a result, the physics and technology of OPRR, power extraction, FW and TC should be first developed on compact devices, rather than on the reactor scale machines. In a comparison of two approaches for compact ignition, i.e., use of high magnetic field or high-beta spherical tokamaks, Ignited STs have a crucial advantage in being able to use up to 90% of neutrons for breeding. Their central rod has a relatively small space view angle for neutrons, thus, leaving most of the space around the plasma available for breeding materials.

This section explains the necessity of high-beta and ignited spherical tokamaks (IST) for the development of reactor physics and technology.

2.1. Ignition criterion

A fusion reactor should be able to reach the "ignition" condition when the energy losses are compensated by the fusion alpha particle heating

$$\frac{E_{\rm pl}}{\bar{\tau}_{\rm E}} = f_\alpha \int P_\alpha \,{\rm d}V, \quad P_\alpha = E_\alpha n_{\rm D} n_{\rm T} \langle \sigma v \rangle_{\rm DT}, \tag{1}$$

$$\frac{E_{\rm pl}}{\bar{\tau}_{\rm E}} \equiv \frac{E_{\rm pl}}{\tau_{\rm E}} + \int P_{\rm rad} \,{\rm d}V, \tag{2}$$

where $E_{\rm pl}$ is the total plasma energy integrated over plasma volume V, P_α the density of the alpha particle power, $E_\alpha = 3.5\,{\rm MeV}$, $n_{\rm D}, n_{\rm T}$ are the densities of deuterium and tritium, respectively, and $\langle \sigma v \rangle_{\rm DT}$ is the cross-section of the reaction. The coefficient f_α reflects the direct losses of the α-particles. In Eq. (2) the energy confinement time $\bar{\tau}_{\rm E}$ (with a bar) takes into account all energy losses from the plasma, including radiation power $P_{\rm rad}$, while, typically, the definition of $\tau_{\rm E}$ excludes the radiation.

Because the cross-section of the DT reaction within the known accuracy is proportional to the plasma temperature squared T^2 [8], the appropriate scaling for the volume averaged alpha particle power can be written as

$$\frac{1}{V_0} \int P_\alpha \,{\rm d}V = C_\alpha \langle 4 p_{\rm D} p_{\rm T} \rangle = \langle p \rangle^2 f_{\rm pk} C_\alpha, \tag{3}$$

$$C_\alpha \equiv \frac{\langle P_\alpha \rangle}{\langle 4 p_{\rm D} p_{\rm T} \rangle}, \qquad f_{\rm pk} \equiv \frac{\langle 4 p_{\rm D} p_{\rm T} \rangle}{\langle p \rangle^2}, \tag{4}$$

where $\langle \cdot \rangle$ stands for volume averaging, V_0 the total plasma volume, $p, p_{\rm D}, p_{\rm T}$ the correspondingly plasma, deuterium and tritium ion pressures, respectively. The coefficient C_α, which depends on T, $p_{\rm D}$, $p_{\rm T}$ profiles, is referred here as a reactivity factor. The "peaking" factor $f_{\rm pk}$ takes into account peakedness of the plasma pressure profile, dilution of DT mix by helium ash and by impurities, and the difference in electron and ion temperatures. In the low recycling regime the content of impurities and contribution of hot α-particle pressure can be made small.

The value of C_α can be calculated for different density and temperature profiles. Here, we introduce the reference normalized profiles shown in Fig. 1a

$$s_\nu(\bar{V}) \equiv (1+\nu)(1-\bar{V})^\nu, \qquad n_{\rm e}(V) = \langle n_{\rm e} \rangle s_{\nu_n}(\bar{V}), \tag{5}$$

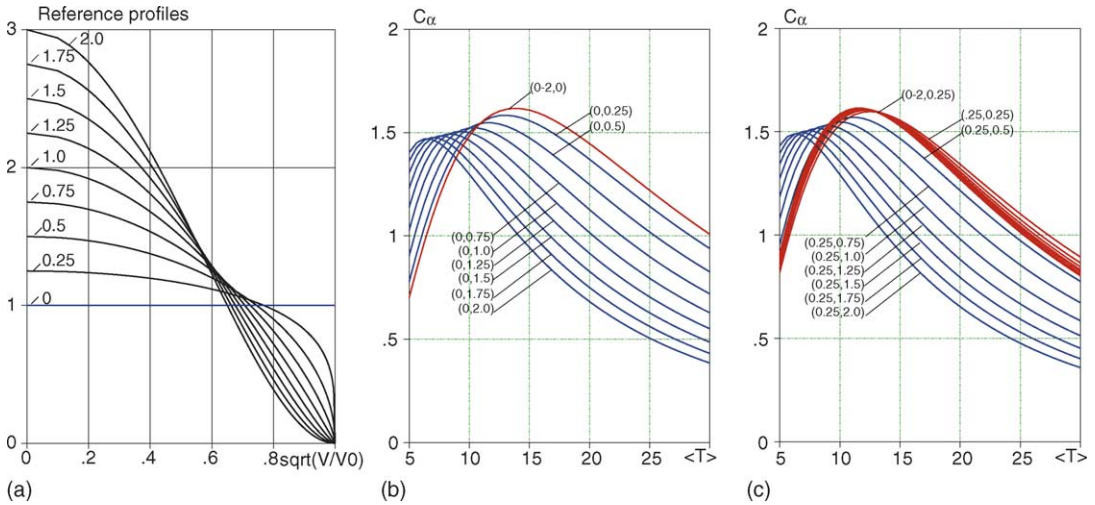

Fig. 1. (a) Reference profiles (with the same volume averaged values) for plasma density and temperature. (b) C_α as a function of averaged plasma temperature. The red curve for $\nu_T = 0$ does not depend on $\nu_n = 0$–2. Blue curves correspond to $\nu_n = 0$ and $\nu_T = 0.25$–2. (c) C_α for another set of profiles. Red curves are for $\nu_T = 0.25$ with $\nu_n = 0.25$–2, and blue curves are for $\nu_n = 0.25$ with $\nu_T = 0.25$–2. For interpretation of the references to color in this figure legend, the reader is referred to the web version of this article.

$$T(V) = \langle T\rangle s_{\nu_T}(\bar{V}), \tag{6}$$

where $\bar{V} \equiv V/V_0$ is the normalized plasma volume. Each pair of density and temperature profiles can be referenced by a double index (ν_n, ν_T).

Fig. 1b and c show the fusion reactivity factor C_α for two sets of profiles each. The red curves corresponds to flat and "almost flat" temperature profiles of the low recycling regime, while blue ones to the high recycling regimes with flat or "almost flat" density. While there is a significant dependence of the C_α factor on the averaged temperature, its maximum value for each profile is almost the same for different profiles. The optimum value, which we refer as $\bar{C}_\alpha$, as a function of temperature peaking index ν_T for different density profiles is shown in Fig. 2a. With good accuracy

$$\bar{C}_\alpha \simeq 1.5\left[\frac{\mathrm{MW}}{\mathrm{MPa}^2}\right]. \tag{7}$$

Note that this optimum value can be achieved only in a stationary regime. Any plasma profile oscillations in time would make the operational C_α smaller than $\bar{C}_\alpha$.

For comparison Fig. 2a shows also an analogous factor $\bar{C}_X$ expressing the Bremsstrahlung radiation $\int P_{X-ray}\,\mathrm{d}V$ [9] in the same form as $\bar{C}_\alpha$

$$\bar{C}_X \equiv \frac{1}{\langle p^2\rangle Z_{\mathrm{eff}} V_0}\int P_{\mathrm{X\text{-}ray}}\mathrm{d}V. \tag{8}$$

The Bremsstrahlung radiation is proportional to Z_{eff} and for $Z_{\mathrm{eff}} = 1$ constitutes less than 10% of the α-power for the optimum temperatures.

The ignition criterion (2) can be now written as

$$\frac{3}{2}\frac{\langle p\rangle}{\bar{\tau}_\mathrm{E}} = f_\alpha\langle P_\alpha\rangle, \qquad \frac{2}{3}C_\alpha\langle p\rangle\bar{\tau}_\mathrm{E} = \frac{1}{f_\alpha f_{\mathrm{pk}}}. \tag{9}$$

The pressure peaking factor f_{pk}, which for reference profiles depends on the sum $\nu_n + \nu_T$, is shown in Fig. 2b. For the optimum choices of the plasma temperatures (7), the ignition criterion is reduced to

$$f_{\mathrm{pk}}\langle p\rangle f_\alpha\bar{\tau}_\mathrm{E} = 1 \quad \text{or} \quad f_{\mathrm{pk}}\langle p\rangle\bar{\tau}^*_E = 1, \tag{10}$$

where the abbreviation $\bar{\tau}^*_E \equiv f_\alpha\bar{\tau}_\mathrm{E}$ is introduced to absorb the factor f_α. The same criterion can be written in equivalent forms

$$f_{\mathrm{pk}}\langle n_\mathrm{e}T\rangle\bar{\tau}^*_\mathrm{E} = 31\times 10^{20},$$

$$f_{\mathrm{pk}}\beta B^2\bar{\tau}^*_\mathrm{E} = 2.5, \quad \beta \equiv \frac{2\mu_0\langle p\rangle}{B^2}, \tag{11}$$

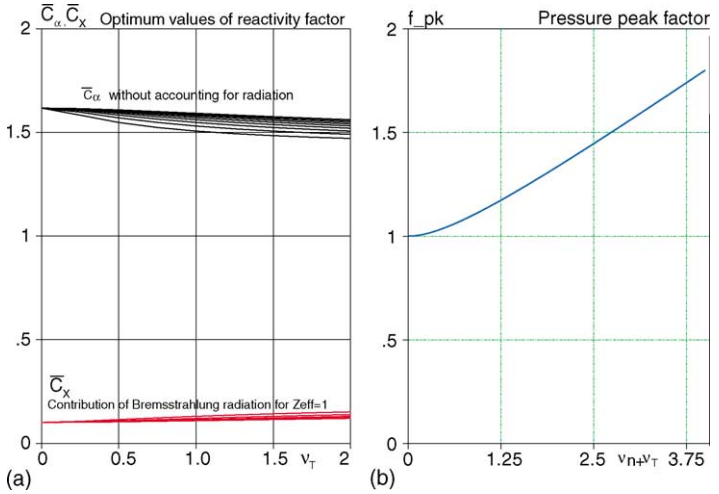

Fig. 2. (a) Optimum reactivity factor $\bar{C}_\alpha$ of alpha particles and Bremsstrahlung radiation factor $\bar{C}_X$ ($Z_{\text{eff}} = 1$) for different reference density and temperature profiles (ν_n=0–2,ν_T=0–2) at optimum plasma temperature. (b) Pressure peaking factor for reference profiles.

where n_e is the plasma density in [m^{-3}], and T is in [keV]. In practice (e.g., ITER applications) another form, written in terms of central values of plasma density n_0 and temperature T_0 (assuming some particular factors f_α, f_{pk}),

$$n_0 T_0 \tau_E = 50 \times 10^{20} \tag{12}$$

is in use (with conventional τ_E not accounting for the radiation).

Ignition criterion (10) should be fulfilled during both ignition phase and power production operation.

This criterion is only a necessary condition. It was obtained under the most optimistic assumptions. Thus, a stationary regime with an optimal plasma temperature is assumed. The high recycling regime with a peaked temperature profile typically exhibits relaxation oscillations, and the criterion (10) should be, in fact, exceeded. Also, the presence of α-particles and impurities in the plasma reduce the peaking factor f_{pk} from its pure plasma value. Recall that radiation losses are hidden in the definition of $\bar{\tau}_E$.

In contrast to ignition, a relaxed notion of a so-called "burning" plasma, when the criterion (10) is not fulfilled, presumes a significant external power for plasma heating comparable to the fusion power. In the case of a power reactor this would conflict with economics, technology and the tritium cycle. Burning plasma would also require higher power extraction from the plasma. On the path to the reactor, the burning plasma has a very limited potential contribution to the reactor development.

2.2. Operational Power Reactor Regime

At the optimum temperature, the total fusion power of the reactor is proportional to the plasma pressure squared

$$P_{\text{DT}} = 5 \int P_\alpha \, \mathrm{d}V = 7.5 V_0 f_{\text{pk}} \langle p \rangle^2 = 1.2 V_0 f_{\text{pk}} (\beta B^2)^2. \tag{13}$$

We note that, e.g., for parabolic pressure, $\nu_n + \nu_T$=1 in Fig. 2b, $f_{\text{pk}} = 4/3$ (or close to 1 because of dilution of DT mixture by impurities and helium). In terms of the energy confinement time it can be written as

$$P_{\text{DT}} = 7.5 \frac{V_0}{f_{\text{pk}} \bar{\tau}_E^{*2}}. \tag{14}$$

This form is essential to the notion of the operational power reactor regime. It shows that power production requires a reduced effective energy confinement time $\bar{\tau}_E^*$ and, correspondingly, enhanced plasma pressure. Thus, for typical $P_{\text{DT}} = 3$ GW for a reactor (assuming 1/3 conversion into electricity and a parabolic plasma pressure) the energy confinement time $\bar{\tau}_E^* = 1$ s leads to a reasonable plasma volume $V \simeq 500\,\text{m}^3$. Energy

confinement times $\bar{\tau}_E^*$ greater than 2 s are essentially not suitable for the power producing phase as they require a plasma volume higher than 2000 m^3.

Given the size and the power of the reactor, the energy confinement time for the operational power reactor regime is determined by Eq. (13) to be typically in the range of 0.8–1.3 s and $\langle p \rangle$ in the range of 0.8–1 MPa.

The relatively small energy confinement time $\bar{\tau}_E^*$ required for OPRR can be comparable with the slowing down time of α-particles [10]

$$\frac{1}{\tau_{sd}} \simeq \left[5.4 - 0.3164 \ln\left(\frac{10\sqrt{n_e}}{T_e}\right)\right] n_e \left(\frac{10}{T_e}\right)^{3/2}. \tag{15}$$

(n_e here is in $10^{20}\,m^{-3}$). As a result, the pressure p_h of the hot alphas could be a noticeable fraction of the plasma pressure

$$\frac{\langle p_h \rangle}{\langle p \rangle} \simeq \frac{\tau_{sd}}{\bar{\tau}_E} = f_\alpha \frac{\tau_{sd}}{\bar{\tau}_E^*}, \tag{16}$$

thus, reducing factor f_{pk} and efficiency of the reactor.

Good confinement with an excessive energy confinement time $\bar{\tau}_E$ would allow for direct losses of hot alpha particles. This would reduce the fraction f_α and contribution of p_h into plasma pressure while keeping $\bar{\tau}_E^*$ appropriate to OPRR.

2.3. Ignition phase

In contrast to OPRR, the ignition parameters are determined by the available auxiliary heating power P_{ext}. The power P_{ext} required for igniting the plasma is determined by the plasma energy balance equation

$$\frac{dE_{pl}}{dt} = P_{ext} - \frac{E_{pl}}{\bar{\tau}_E} + f_\alpha P_\alpha > 0. \tag{17}$$

Without P_{ext} this equation has two stationary solutions: $E_{pl} = 0$ and $E_{pl@ign}\bar{\tau}_{E@ign} = f_\alpha P_{\alpha@ign}$, where index '@ign' refers to the ignited state. With the external power present, these two solutions approach each other and merge at some level of P_{ext}, corresponding to the minimum external power necessary for ignition.

Assuming the best possible scenario where the temperature profile is kept optimal while P_α is externally controlled (e.g., by the density level) the energy balance equation can be rewritten in a normalized form

$$\bar{\tau}_{E@ign}\frac{d\bar{E}}{dt} = \frac{P_{ext}}{f_\alpha P_{\alpha@ign}} - \bar{E}\frac{\bar{\tau}_{E@ign}}{\bar{\tau}_E} + \bar{E}^2 > 0, \tag{18}$$

$$\bar{E} \equiv \frac{E_{pl}}{E_{pl@ign}},$$

$$P_\alpha = \frac{E_{pl}^2}{E_{pl@ign}^2} P_{\alpha@ign} = \bar{E}^2 P_{\alpha@ign}. \tag{19}$$

Parameters at the ignited state were used here for normalization. If $\bar{\tau}_E = \bar{\tau}_{E@ign}$ independent of the heating power is assumed, this equation gives the estimate for the minimum necessary external power

$$P_{ext} > \frac{1}{4} f_\alpha P_{\alpha@ign} = \frac{1}{20} f_\alpha P_{DT@ign},$$

$$\bar{\tau}_{E@ign} > \sqrt{\frac{1.5 V_0}{4 f_\alpha P_{ext}}}. \tag{20}$$

Such a level provides the positiveness of the right hand side in the energy balance equation.

Even with the small factor 1/20 in front of P_{DT}, this expression indicates that it is impractical to ignite the plasma at the operational point of the reactor, where $P_{DT} \simeq$ 3–4 GW. It would require 150–200 MW of installed axillary heating power working only for a short time during the ignition phase.

Instead, the ignition should be performed at enhanced energy confinement time $\bar{\tau}_{E@ign}$, which would be 2–2.5 times higher than the operational $\bar{\tau}_E$. Accordingly, the beta value is reduced at the ignition phase.

Ignition phase is distinct from OPRR and requires an enhanced energy confinement time $\bar{\tau}_{E@ign}$ determined by Eq. (20) on the basis of an available auxiliary heating power P_{ext}.

The power reactor should be consistent with both ignition and OPRR, which have in common the same ignition criterion but different contributions from its factors. Accordingly, the transition from ignition phase to OPRR would require only a restricted, in accordance with Eq. (14), energy confinement degradation $\tau_E \propto 1/\sqrt{P_\alpha}$ when the fusion power increases.

Conventional regimes contain a fundamental problem in making transition from ignition to OPRR. The ion-temperature gradient (ITG) turbulence, associated with low edge temperature, preserves the core temper-

ature gradients by enhancing energy losses and degrading the confinement [3]. The turbulence makes the temperature profile depend only on its edge value.

In the reactor, because of the necessity an optimal (for fusion power) level of core temperature and a low edge temperature (for power extraction in the diverter) its profile should be essentially unchanged during the transition. An increase in density provides an increase in power. Based on this model, the expected scaling would be $P_\alpha \propto n^2$, $E_{pl} \propto nT \propto n$, and $\tau_E \propto n^{-1} \propto P^{-1/2}$, just marginal to the requirement.

The problem is that during transition from ignition to OPRR the fusion power should be raised by a factor of $\simeq$10 and the model of "transport enhancement by turbulence" is unlikely to be applicable. At some level of power, “transport” most probably will be replaced by bursting phenomena and then, by macroscopic relaxations and loss of confinement.

The consequences of an intrinsically turbulent regime for energy confinement at power levels far exceeding the critical level for instability are unpredictable. In any case, they will degrade the “expected marginal” scaling of τ_E versus power, thus, preventing conventional plasmas, even ignited, from transition to OPRR.

The high edge temperature of the low recycling regimes can eliminate (or control) the ITG-turbulence, thus, raising expectations for both ignition and OPRR.

2.4. Fusion power is needed for development of OPRR

Separation of ignition and OPRR is clearly seen on the plot “fusion power versus energy confinement time” $\overline{\tau}_E^*$ in Fig. 3a. Recall that $\overline{\tau}_E^*$ accounts for all losses including radiation and loss of α-particles.

The black curve is the total fusion power P_{DT}, while the red one is P_α. The green line shows the level of $P_{ext} \simeq 30$ MW, necessary for ignition. The dashed green line is $4P_{ext}$. Its intersection with P_α determines the ignition parameters. The blue curve gives the β-value (scale on the right side) necessary to meet the ignition criterion (11). The dashed black curve in the low-right corner shows P_{DT} for the ITER volume $V = 834\,m^3$.

For a reactor-like plasma size, $V = 400\,m^3$ (Fig. 3a), the ignition phase is well separated from OPRR. Separation becomes bigger for larger volumes. The dashed blue curve in Fig. 3a shows a scenario path, starting with plasma heating by external power, then ignition and transition to OPRR.

The ignition phase should last only several energy confinement times, while the operational regime is continuous and has much more challenging plasma parameters.

The high pressure plasma of OPRR ($\langle p\rangle \simeq$ 0.8–1 MPa) can be developed only with use of fusion power as the dominant heating power.

The heating power P_α of OPRR (13), e.g., assuming a parabolic pressure ($f_{pk} = 4/3$, $\langle p\rangle = 0.8$–1 MPa),

$$P_\alpha \simeq 1.5 f_{pk}(0.64\text{–}1)V_0 \simeq (1.3\text{–}2)V_0 \quad (21)$$

would be too large even for a plasma volume of 50 m^3 (TFTR size). Substituting for P_α would require 65–100 MW of external power (twice the TFTR auxiliary power) in order to reach and sustain the OPRR. Shielding would lead to further enlargement of the plasma volume and to a higher power. The available plasma heating methods simply cannot provide the power for simulation of OPRR.

Only compact machines, like ST, with a smaller volume $V_0 \simeq 30\,m^3$ and no shielding of the central rod can potentially reach the OPRR level of $\langle p\rangle$, and develop the regime with much less reliance on fusion power. At the same time, as discussed later, ignition still will be required for the purpose of developing the FW design.

While for large machines ignition and OPRR are separated, it may be possible to ignite an ST at the relatively small energy confinement time of OPRR. The (P-$\overline{\tau}_E^*$) diagram for such an ignited ST (IST) with plasma volume $V = 30\,m^3$) is shown in Fig. 3b. With a reasonable $B = 3$ T (assuming no shield on the central rod) and total fusion power of about 0.5 GW, it can be ignited with $P_{ext} \simeq 25$–30 MW reaching $\beta = 0.4$–0.45 at the OPRR point. For conventional plasma $\beta < 0.04$, this diagram would require a device with, at least, three times higher magnetic field.

2.5. Cost estimates of electricity produced

The monetary value of the electricity produced W_{Electr} during the life time of the reactor is limited. Assuming 30 years of uninterrupted operation, a refer-

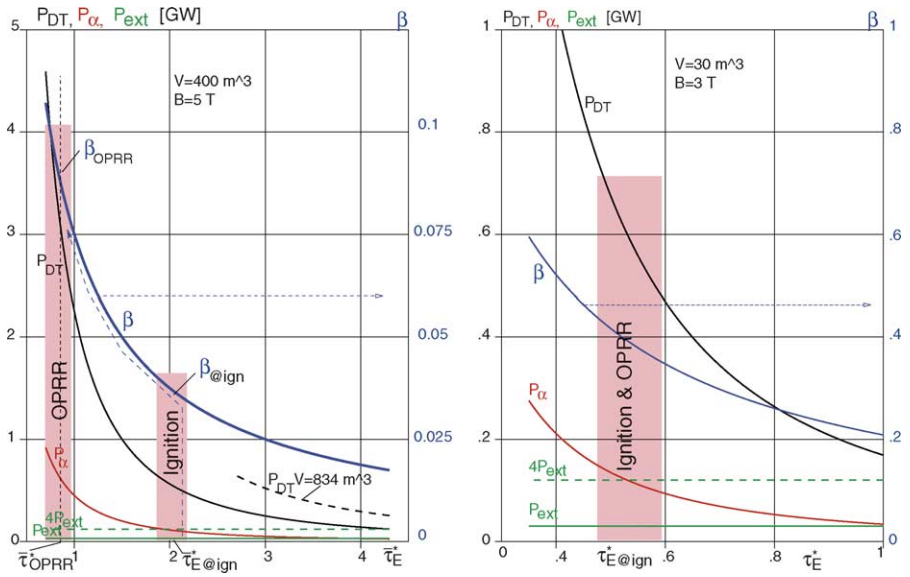

Fig. 3. Fusion power vs. cumulative energy confinement time $\bar{\tau}_E^*$ for (a) a reactor with $B = 5\,\mathrm{T}$ and $V = 400\,\mathrm{m}^3$, and (b) for an ignited spherical tokamak with $B = 3\,\mathrm{T}$ and $V = 30\,\mathrm{m}^3$.

ence estimate can be written as

$$W_{\mathrm{Electr}}[\$\mathrm{B}] = 10.5 P_{\mathrm{Electr}} \frac{C_{\mathrm{kWh}}}{0.04}, \tag{22}$$

where P_{Electr} [GW] is the electric power of the reactor, e.g., $P_{\mathrm{Electr}} \simeq P_{\mathrm{DT}}/3$ and C_{kWh} is the cost of 1 kWh.

The cost of the reactor should be only a fraction of the monetary value of electricity produced, e.g., given by Eq. (22).

Although extremely simplified even such an estimate imposes severe restrictions on the cost of the fusion reactor itself, its operation and maintenance. Given the \$5 B cost of the 0.4 GW ITER, it suggests that the power reactor, in approximately half of the ITER plasma volume, should have an order of magnitude higher fusion power. Clearly, the conventional plasma does not fit the simplest cost considerations.

2.6. Cost estimate of first wall replacement

The first wall is the most challenging structural element of a reactor, which imposes additional constraints on the reactor physics regime and design. The necessity of using fusion power for its development ties the technology of the FW with plasma physics at the very early stage of development of OPRR and the FW.

Periodic replacement of the first wall surface (if it is based on solid materials) leads to additional expenses for operation of the fusion reactor. The characteristic neutron fluence for the FW life time is about 15 MW year/m^2. It can be converted into the corresponding value C_{FW} of electricity "produced" per 1 m^2 during the life time of the FW element

$$C_{\mathrm{FW}} \left[\frac{\$\mathrm{B}^2}{\mathrm{m}}\right] \simeq 0.001 \frac{5.25}{3} \frac{C_{\mathrm{kWh}}}{0.04}, \tag{23}$$

where $1/3$ is assumed as a conversion factor of fusion power to electricity.

The cost of replacement of the first wall surface should be within the limit C_{FW} given by Eq. (23).

This requirement strongly motivates new approaches for the first wall design with emphasis on low activation structures and liquid elements (liquid lithium, FLiBe, Be, etc.). Correspondingly, the plasma regime should be consistent with these innovative structures of the first wall. In this regard, the low recycling regime is compatible, e.g., with the flowing lithium wall surface [11], although it requires solving the problem of pumping the helium ash.

2.7. Tritium consumption and FW development

While it is difficult to assess the total amount of tritium required for development of OPRR, the tritium consumption $W_{T,FW}$ for development of the first wall is straightforward to calculate, and for 15 MW year/m^2 is given simply by

$$W_{T,FW}\left(\frac{kg}{m^2}\right) = 1.046. \quad (24)$$

Such a large consumption of tritium automatically requires breeding tritium with efficiency close to or exceeding 100%.

Three elements of magnetic fusion, i.e., OPRR, FW and tritium cycle are all linked together by the requirement of 100% tritium breeding starting from an early stage of development of a fusion reactor.

Reactor size machines are not suitable for such a triple-goal R&D. Thus, for accumulation of a fluence to the wall of 15 MW year/m^2, a configuration of the size of ITER would consume about 600–700 kg of tritium, far exceeding any foreseeable amount of potentially available non-fusion tritium (about 25 kg in the next three–four decades).

2.8. IST based component test facility is required for reactor R&D

Intrinsic link between OPRR, FW and TC, use of fusion power and high tritium consumption create a situation when the development of the reactor requires compact intermediate devices or a component test facility (CTF), which would be capable of accumulating the necessary neutron fluence and developing FW and TC.

Even in compact devices, like spherical tokamaks (e.g., $V_0 \simeq 30\,m^3$, FW surface $S_{FW} \simeq 55\,m^2$), the tritium consumption would be a big issue and full tritium breeding is required. Thus, rather than being a "driven" device, the CTF should be a mini-reactor working at OPRR plasma parameters, almost full FW functionality, and closed TC. The only difference from the power reactor would be simplification of shielding (with some structure exposed to neutrons) and absence of electricity production. With such a simplification the CTF could be realized in a form of IST.

Fig. 4 shows the neutron coverage fraction, or NCF (surface fraction weighted using influx of primary fusion neutrons) of the central column as a function of plasma aspect ratio. Although actual losses of neutrons depend significantly on detail and materials of the design, NCF is one of the primary factors, contributing to losses. Based on NCF, STs have significant advantage with respect to conventional aspect ratio devices targeting CTF requirement. The central rod in the ST has a minimal averaged space angle compared to other toroidal configurations.

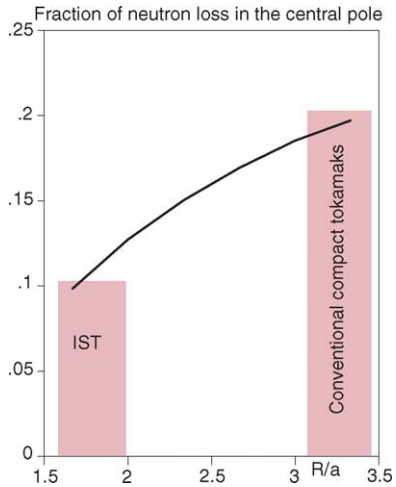

Fig. 4. Neutron coverage fraction of the central pole as a function of aspect ratio. (Plasma cross-section of IST in Section 6, Fig. 9 was used for calculations.)

At the same time, the CTF, even based on an ST, may have an unacceptable level of neutron losses if the ports for neutral beams are not filled with tritium breeding material. In order to use this reserve, plasma in CTF should be ignited and all NBI ports should be covered with the breeding material.

Note that ignition, which is motivated by tritium breeding considerations, is not an excessive requirement for IST also from the plasma physics point of view. In contrast to conventional plasma, STs in the LiWall regime are not severely limited in β. The "burning" plasma is close to ignition anyway, and there will be no substantial plasma physics obstacles between "burning" and ignition in ST.

Among fusion configurations ignited spherical tokamaks are uniquely positioned for development of OPRR, FW and TC for fusion reactor.

The geometry of the ignited ST together with the ignition regime allows the maximum use of the FW surface for tritium breeding.

2.9. Transition from CTF to the power reactor

On the way to the reactor, first, the OPRR plasma regime should be developed (probably with limited or no breeding of tritium). While the plasma pressure of OPRR can be potentially achieved in two types of compact machines: IST or high-field conventional tokamaks, only ISTs are consistent with the following development of FW and TC.

The way to fusion power reactor includes, first, achieving OPRR plasma parameters on LiWall IST, second, a phase of development of FW and TC on IST based CTF, and then transition to the reactor itself.

Thus, the IST and its CTF phase should bear the major part of practical fusion development. Essentially, ISTs could demonstrate all three objectives of magnetic fusion and would represent the most crucial step toward the fusion reactor. Then the transition to a power reactor will require changing the plasma geometry (to conventional aspect ratio), developing the full functionality of the FW (including high grade heat extraction from the blanket), and full shielding of the neutron zone. Other changes (e.g., superconducting coils, heat conversion into electricity, etc.), are supplementary to these reactor core transformation.

Improvements of the present plasma parameters, its stability and confinement would require, first of all, making a transition to the high edge plasma temperature and solving associated plasma boundary problems. Lithium covered stabilizing walls (e.g., copper with either solid, molten or liquid Li surface and a special interface layer) positioned right at the plasma boundary and complemented with the power extraction system suggest a practical approach for developing the IST grade plasma. At the R&D stage the physics of the new regime does not require intense lithium flows.

3. Basics of plasma confinement in the low-recycling regime

With respect to the boundary conditions and to plasma fueling two kinds of plasma regimes can be distinguished in quasi-stationary configurations: high- and low-recycling. In the first one, the plasma is refueled by neutral gas through the boundary, while in the second, the boundary is pumped out, while the neutral particles are supplied into the core itself (either by neutral beams or by pellet injection).

With the boundary localized particle source, the particle confinement time near the edge is small, leading to intense mixing of plasma particles at the edge. As a result, the edge plasma temperature is relatively low compared to its core value. The temperature profile is peaked, while the density profile is flattened.

In the second case with core fueling, the particle confinement time corresponds to the core confinement. If the plasma is well pumped from the edge, the wall and its temperature are not "visible" to the plasma. As a result, a high plasma edge temperature, comparable with its core value is established when the plasma particles are gradually heated while diffusing through the core toward the boundary. The temperature profile becomes flattened or hollow, while the density profile is peaked in accordance with the position of the particle source.

Both situations are described by the following boundary condition for the energy transport equation

$$\gamma \Gamma^{\text{micro}}_{\text{edge}\to\text{wall}} T_{\text{edge}} = \int P_{\text{heat}}\, \mathrm{d}V, \tag{25}$$

written for each species of the plasma (convection coefficient $\gamma = 5/2$ for Maxwellian plasma). Here, $\Gamma^{\text{micro}}_{\text{edge}\to\text{wall}}$ is the particle (microscopic) flux toward the wall, T_{edge} is the edge temperature, P_{heat} is the density of heat source, $\mathrm{d}V$ is the plasma volume element.

In the high recycling case the plasma particles are resupplied to the edge after collisions with the wall surface. In this case, $\Gamma^{\text{micro}}_{\text{edge}\to\text{wall}}$, which is the directed plasma particle flux to the wall, is much large than the particle diffusion (macroscopic) flux inside the plasma. As a result, the edge temperature is low compared to the core temperature

$$\Gamma^{\text{micro}}_{\text{edge}\to\text{wall}} \gg \Gamma_{core},$$

$$T_{\text{edge}} \simeq \frac{1}{\gamma \Gamma^{\text{micro}}_{\text{edge}\to\text{wall}}} \int P_{\text{heat}}\, \mathrm{d}V \ll T_{core}. \tag{26}$$

This formula is approximate to the extent that the energy of the particles in the edge localized source was neglected with respect to the core temperature. Also, due to possible non-Maxwellian distributions the γ coefficient in the convective energy flux can be different from $5/2$.

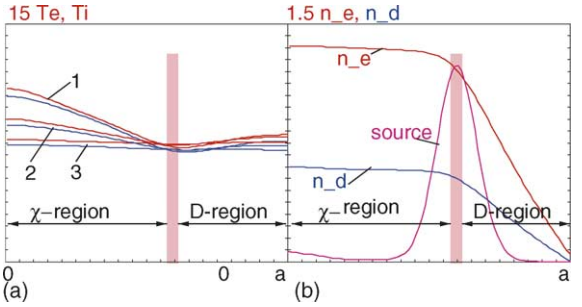

Fig. 5. χ- and D-confinement regions in the low recycling regime. (a) Electron and ion temperatures for three values of thermo-conduction coefficients, related to each other as $\chi_2 = 2\chi_1$, $\chi_3 = 10\chi_1$ (index is the curve number on the plot), and same particle diffusion. (b) Electron, ion (deuterium) density and localization of the particle source.

In the low recycling case all particles are absorbed by the wall and "microscopic" flux is equal to "macroscopic" one

$$\Gamma^{\mathrm{micro}}_{\mathrm{edge}\to\mathrm{wall}} \simeq \Gamma_{core},$$

$$T_{\mathrm{edge}} = \frac{1}{\gamma\Gamma_{core}} \int P_{\mathrm{heat}}\,\mathrm{d}V \simeq T_{core}. \tag{27}$$

The plasma energy, essentially, is not affected by the wall and the edge temperature reaches its natural level, comparable or exceeding the core temperature. Instead, the density at the edge becomes very low (thus, eliminating the Greenwald density limit [7]). In the low recycling case, it is possible to expect a less turbulent (or stabilized at high beta of IST) plasma, where the rate of convection is described by a factor $\gamma \simeq 5/2$.

Two confinement regions are present in the plasma for the case of core fueling and pumping walls, as is shown in Fig. 5. With respect to the position of the core particle source, there are different contributions from convective (or particle diffusion term) and thermo-conduction q_χ energy transport into the total energy flux Q

$$Q = \frac{5}{2}\Gamma T + q_\chi = \int_0^V P_{\mathrm{heat}}\,\mathrm{d}V. \tag{28}$$

Outside the localized particle source, the temperature profile relaxes to its natural level, when the particles acquire energy from the heating source, while diffusing toward the wall. As a result, the temperature profile is hollow in this region, referred to here as the D-region. The energy losses here are determined solely by the particle diffusion, $q_\chi \ll 5/2\,\Gamma T$. Thermo-conduction tends to make the profile flat and, thus, returns some energy from the boundary into the core.

Inside the localized source, the situation is the same as in the conventional regime, where the plasma density is flattened, the convective losses are small and the energy transport is dominated by thermo-conduction, $q_\chi \gg 5/2\,\Gamma T$. A peaked temperature profile is established in this region, referred to here as χ-region.

The D-region is the key feature of the low recycling regime, having different and, potentially much improved, confinement properties than the conventional plasma. First, because of ambipolarity, the energy losses in the D-region are determined by the best confined plasma component and are less sensitive to thermo-conduction than in the χ-region. A comparison of cases with 3 values of thermo-conduction coefficient in Fig. 5a shows that the only effect of significantly (10 times) enhanced thermo-conduction is a small change in the temperature profile.

Experimentally, there are indications that reduced recycling leads to improved confinement. Thus, all TFTR high performance regimes were achieved with "lithium conditioning", resulting in reduced recycling [12] (although explained within conventional ITG theory [13]). The most prominent results with high plasma temperature and enhanced edge pumping have been obtained on DIII-D in a quiescent double barrier regime [14], demonstrating good confinement and a stable plasma.

Theoretically, the presence of the D-region creates a special situation for the confinement, not studied yet in the tokamak research. Although there are no theory simulations of turbulent transport in the low-recycling regime, which would give a corresponding transport model, theory unambiguously concludes that an increase in the edge temperature improves the core confinement [2].

As an example, ASTRA code calculations of low recycling plasma performance using the PPPL-IFS transport model [15,16] for ITER-FEAT tokamak are shown in Fig. 6 with boundary conditions (27) and $\gamma = 3$. The core fueling was simulated by a particle source S_n localized at 0.5 m from the plasma edge (Fig. 6a). A substantial temperature pedestal, $T_{\mathrm{i}}(a) \simeq 10$ keV, develops at the edge, and the entire plasma cross-section produces the fusion power. The ITER plasma would be ignited (Fig. 6b) if such a low recycling regime could be es-

tablished. In simulations, the low recycling regime has been "started" at some time from a stationary standard ITER plasma. After establishing a high edge temperature at $t = t_0$, its fusion power increases in calculations (Fig. 6b), tripling the reference value of 400 MW.

The expected enhanced confinement in the low recycling plasma, its presumably, smaller sensitivity to turbulence and to the heating power [12] could make the LiWall regime suitable for the OPPR and its development path. Moreover, as it is shown later, in spherical tokamaks the residual micro-instabilities, i.e. electron trapped modes, can be stabilized in the D-region at sufficiently high plasma beta. This would lead, potentially, to neo-classical confinement and open the possibility for reaching even D^3He (or ^3He "catalyzed DD") fusion.

Note, that in the ITER-FEAT example of Fig. 6, the high fusion performance was solely a result of the increased volume of plasma participating in fusion. The diffusion model used in simulation includes $\propto 1/n_e$ diffusion coefficient, leading to a sharp drop of density near the edge, enhanced particle flux in the D-region and energy loss. Such a diffusion model, in fact, prevents better confinement despite elimination of the thermo-conduction energy loss. At the same time, for the low recycling regime there is no real justification for such a $\propto 1/n_e$ diffusion model, which originated from the global energy (not the particle) confinement scaling obtained for much higher plasma density.

Control of the temperature pedestal in the low recycling plasma regime would give an unambiguous test of existing thermo-conduction models as well as unique information on the diffusion properties of the plasma.

4. Particle and power extraction by close-fitting LiWalls

Exceptional properties of pumping hydrogen plasma particles by lithium have been observed in tokamaks during the very first experiments involving a large area of lithium coated wall surface on T-11 [17–20] and with rail [21] and toroidal liquid lithium limiter [22,23] on CDX-U spherical tokamak.

An assessment of the pumping capacity of the lithium surface can be made using a rather realistic

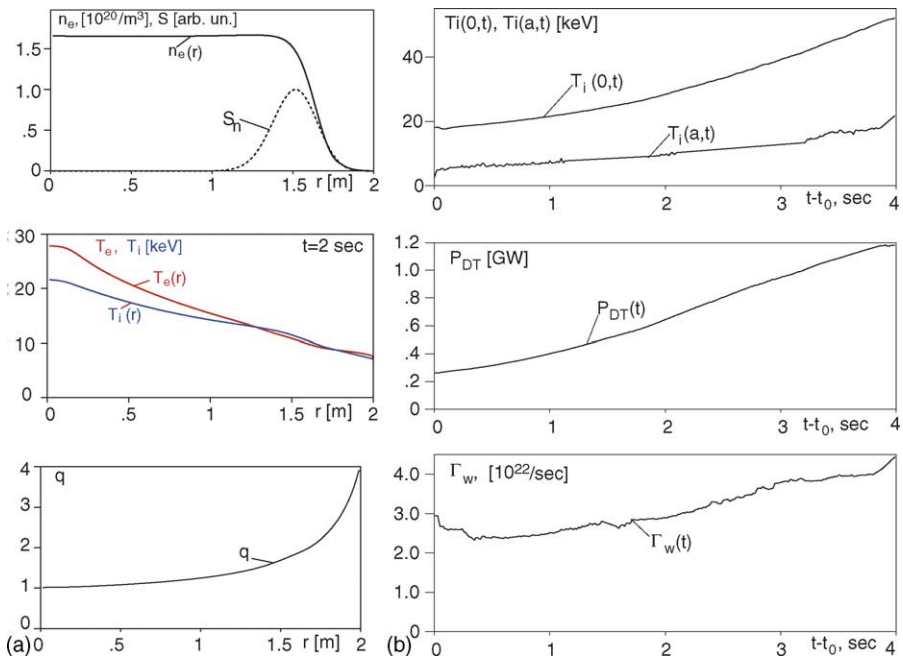

Fig. 6. (a) Plasma radial profiles: core localized particle source S, electron n_e density, electron T_e and ion T_i temperatures, and q profiles as functions of the minor radius. (b) Time evolution of central $T_i(0)$ and edge $T_i(a)$ ion temperatures, fusion power P_{DT} and the particle flux to the wall Γ_w.

assumption that Li can absorb the hydrogen atoms essentially at the ratio 1/1 with respect to the Li atoms. According to TRIM code calculations (J.P. Allain, University of Illinois), in solid lithium about 150–200 mono-layers of Li (for energy of the hydrogen atoms of 2 keV) can work for pumping. In liquid or molten Li, macroscopic depths are involved due to thermal diffusion. Accordingly the pumping capacities $C_{\rm pump}^{\rm Li}$ for these two cases are characterized by

$$C_{\rm pump}^{\rm solid\ Li} \simeq 27\frac{10^{20}}{1\,{\rm m}^2},$$

$$C_{\rm pump}^{\rm molten\ Li} \simeq 46{,}000\frac{10^{20}}{1\,{\rm m}^2\times 0.1\,{\rm mm}}. \quad (29)$$

Relatively small amounts of either solid or molten Li (utilizing thermal mixing of the particles inside the layer) on the wall surface are required for plasma pumping. For 1 h of continuous operation of the ITER sized plasma, for example, only 2 L of molten lithium (or 20 m^2 of the surface coverage by 0.1 mm thick molten lithium) would be necessary.

The pumping capacities of a lithium surface far exceed what is necessary for absorbing the plasma particle flux, thus allowing different arrangements for the LiWalls, including coating (micron thin solid Li), "painting" (tens of microns molten Li), gravity or electromagnetically driven boundary layer flow (fraction of mm liquid Li with velocity in the range of cm/s) or electromagnetically propelled liquid lithium flow (fraction of cm thick layer with about 10–20 m/s speed).

The power extraction requirement is that the heat load to the lithium surface should be distributed in order to prevent heating the free Li surface to above 400 °C. Near this temperature the evaporation rate $\Gamma_{\rm Li}$ of Li can be approximated as

$$\Gamma_{\rm Li} \simeq 3\times 10^{20}\,{\rm e}^{\frac{T-400\,^\circ{\rm C}}{50\,^\circ{\rm C}}}\frac{1}{{\rm m}^2\,{\rm s}} \quad (30)$$

and is comparable with expected particle flux from the reactor 2–3×10^{20} $({\rm m}^2\,{\rm s})^{-1}$. Note, that comparable or even modestly exceeding surface source of Li (with small particle confinement time) cannot compete with the core fueling of the plasma and, thus, contaminate the plasma. (This contrasts with the conventional situation when both plasma particle and impurities have the edge localized source.) Nevertheless, the exponential dependence of evaporation on wall temperature essentially establishes the evaporation limit at approximately 400°. Also, it makes the plasma sensitive to potential "hot" spots at the wall.

At the same time, evaporation does have an effect on the particle flux to the wall, and, thus, on the edge plasma temperature, as was explained in the previous section, Eq. (26). In this regard, strong dependence of Li evaporation on the wall surface temperature suggests a straightforward way to control the confinement regime by affecting evaporation and the edge plasma temperature.

Sputtering, as another source of contamination by Li, cannot contribute significantly into contamination because it corresponds to the edge Li source, which is only a fraction of the core source of plasma particles. Also, at plasma temperatures higher than 500 eV, sputtering is degraded with plasma temperature.

Regarding Li edge source control, a copper shell is an excellent material behind the lithium layer, which can provide (even with no active cooling) an exposure time given approximately by

$$t_{\rm exposure} \simeq \frac{d^2}{4D}\begin{cases}\pi\left(\dfrac{\Delta T_{\rm wall}}{T_1}\right)^2 & \text{if } \dfrac{\Delta T_{\rm wall}}{T_1} < \dfrac{2}{\pi},\\ 4\dfrac{\Delta T_{\rm wall}}{T_1}-\dfrac{4}{\pi} & \text{if } \dfrac{\Delta T_{\rm wall}}{T_1} > \dfrac{2}{\pi},\end{cases} \quad (31)$$

where, d is the thickness of the wall, $q_{\rm wall}$ is the energy flux to its surface, $\Delta T_{\rm wall}$ is the allowable temperature increase, and T_1 and D are defined as

$$T_1 \equiv d\frac{q_{\rm wall}}{\kappa_{\rm T}}, \qquad D \equiv \frac{\kappa_{\rm T}}{\rho c_p}, \quad (32)$$

with $\kappa_{\rm T}$, ρ, c_p being the thermoconduction coefficient, mass density and specific heat of the wall, respectively.

The combination of lithium layer and copper wall ($\kappa_{\rm T}\simeq 393$, $\rho = 8960$, $c_p = 400$ in SI units) would allow a reactor relevant heat flux $q_{\rm wall}\simeq 2\,{\rm MW/m^2}$ (an order of magnitude larger than, e.g., in ITER) for 10–30 s ($d\simeq 5$ cm, $\Delta T_{\rm wall}\simeq 400\,^\circ$C) with a stabilizing highly conducting shell right at the plasma boundary. Li and copper is a unique combination suitable for development of the plasma physics aspects of OPRR.

Flowing lithium requires high velocities in order to withstand the reactor relevant power fluxes to the wall

$$\Delta T_{\rm Li} = 200\,^\circ{\rm C}\frac{q_{\rm wall}}{3.5\,{\rm MW/m^2}}\sqrt{4t_{\rm exposure}},$$

$$d_{\rm skin}\,({\rm mm}) = 4.8\sqrt{4t_{\rm exposure}}, \quad (33)$$

where d_{skin} is the thickness of the heat absorbing surface layer. For $q_{wall} \simeq 3.5\,MW/m^2$ it gives 1/4 s of exposure time, corresponding to a velocity $V \simeq 20\,m/s$ and the working layer $d_{skin} \simeq 5\,mm$. Intense lithium streams, driven by magnetic propulsion have the necessary properties [11] and should be developed for such a case.

All the options listed above for reactor relevant heat fluxes require a lithium surface well aligned with the plasma. At smaller heat flux, as well as at lower beta (when the conducting shell is not required), other possibilities may exist. Even a diverter plasma, according to experiments, is interacting with the wall due to so-called "blob" transport mechanism [24,25]. This would suggest effective pumping of the plasma by the Li wall surface even in a diverter configuration.

5. Stability of LiWall limited plasma

A flattened temperature profile, beneficial for energy confinement, results in a flattened current density profile j with a current pedestal at the plasma edge, $j_{edge} \neq 0$. Also, at high betas, which are necessary for OPRR, the bootstrap current makes a significant contribution to the plasma current density. The bootstrap current j_{BS}, which is proportional to the plasma pressure gradient, $j_{BS} \propto p'$, also leads to the current density pedestal at the edge.

With the plasma boundary separated from the conducting wall, the current edge density pedestal further reduces the stability of conventional plasma regimes. The suggested so-called "profile control" for tailoring the current density distribution in order to improve stability remains speculative for reactor power levels.

LiWalls can change the stability situation in tokamaks in a crucial manner by allowing for a conducting wall positioned right at the plasma boundary and, potentially, for eliminating the free boundary instabilities. This allows utilization of the high beta of the second stability regime resulting from a flattened (or reversed) current density profile. Thus, the properties of LiWalls justify a new parameter in stability optimization, i.e., the current density pedestal in conjunction with the fixed boundary plasma, as shown in Fig. 7.

The blue curve in Fig. 7 indicates the β stability limit for TFTR-like circular tokamak geometry, while two black curves are β-limits for elongated plasma

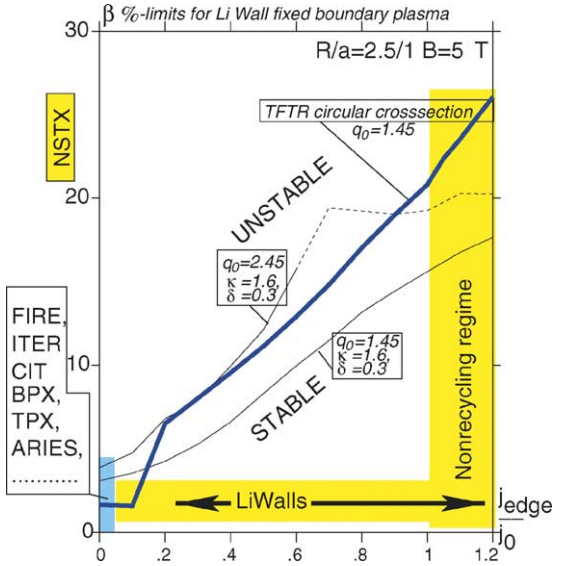

Fig. 7. Stability diagram for fixed boundary plasma with a current density pedestal. (Calculated using ESC, DCON, PEST and BALLOON stability codes for $n = 1, 2, 3, \infty$ MHD modes.)

with the same aspect ratio and for two different values of central q. First, there is a dramatic enhancement of stability β-limits, compared with the conventional plasma when the current density pedestal becomes comparable with the central current density. Second, the plasma shape becomes less important for stability in the low recycling regime. For both circular and non-circular configurations, nearly flat current density profiles have β-limits higher than required for OPRR.

Conventional plasmas with peaked temperature and the current density profile, even with hypothetical stabilization of free boundary modes by some plasma physics mechanisms (e.g., by plasma rotation), would remain entrapped in the "first stability" regime, insufficient for OPRR.

Fig. 8 illustrates the difference in stability properties of peaked and flat current density profiles with the fixed plasma boundary. The first two configurations (marginally unstable) have a peaked current profile. Their pressure gradient is limited in both the center and at the edge, thus, requiring "profile control" for stability optimization. The third configuration has a flat current density, much higher beta limits and is less sensitive to the pressure profile.

It is a unique property of LiWall regimes that flattened temperature and current together with pumping

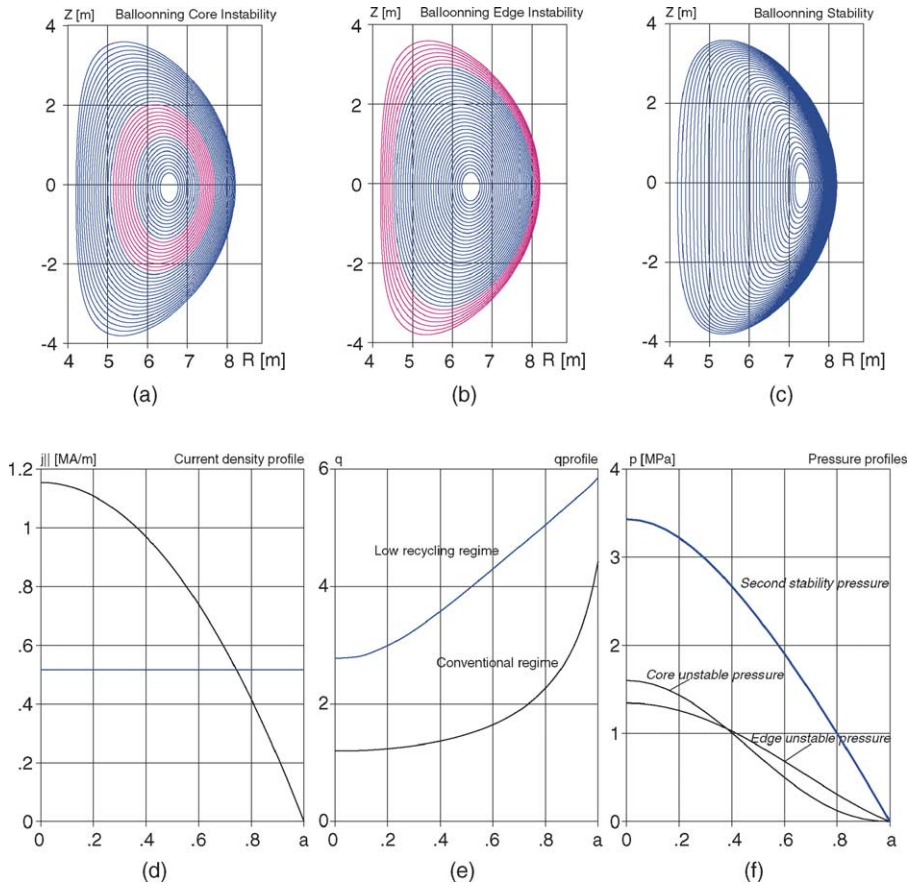

Fig. 8. Magnetic configurations and plasma profiles for "first" and "second" stability regimes. (a) Core ballooning unstable $\beta = 4.6\%$ configuration with a peaked pressure profile. Pink color shows ballooning instable region. (b) Edge ballooning unstable $\beta = 5.3\%$ configuration with a flattened pressure profile. (c) Second stability with $\beta = 16\%$. (d) Current density profile $j_{\|}(a)$, black for configurations (a, b) and blue for configuration (c). (e) Corresponding $q(a)$-profiles. (f) Pressure profiles $p(a)$, black for configurations (a, b) and blue for (c). For interpretation of the references to color in this figure legend, the reader is referred to the web version of this article.

and a stabilizing wall are consistent with each other. The expected enhanced confinement and β limits may satisfy two of the most important requirements of the reactor OPRR. In addition, in the LiWall environment the bootstrap current, enhanced by high-β, does not reduce the ideal plasma stability as it would happen with conventional free boundary plasma.

6. Ignited spherical tokamaks

Spherical tokamaks are the leaders in achieving the highest $\beta \simeq 0.35$ values at a good, tokamak range, energy confinement time [26]. Earlier in the paper additional reasons why STs are unique for developing the magnetic fusion were revealed.

The value of the magnetic field is rather restricted in spherical tokamaks by limitations in space for the central rod of the toroidal magnetic coils. In the case of ignition, there is no possibility of using superconductivity for toroidal coils. Also, it is problematic to rely on the central solenoid for current excitation in an ignited ST.

The low recycling regime and stabilization of the free boundary instabilities by LiWalls open a wide parameter space for ignited operation with OPRR plasma parameters and self-sufficient bootstrap current. Here, we show that the high β limit in low recycling STs

compensates for the relatively low value of the magnetic field and makes an ignited ST feasible.

Concerning the bootstrap current, high β and second stability make two situations possible, (a) when plasma is overdriven with the bootstrap current, and (b) when the configuration is essentially maintained by the bootstrap current. Thus, ignition can be initiated at the lower plasma current and then, the configuration will slowly evolve to the stationary state due to only bootstrap current drive.

6.1. Ignition conditions for IST

In the following examples, the low recycling regime was simulated by a flat temperature $T_e(a) = T_i(a) = 15\,\text{keV}$, where a is radial coordinate related to the toroidal magnetic flux Φ

$$a \equiv \sqrt{\frac{\Phi}{\Phi_0}} \tag{34}$$

(Φ_0 is the total toroidal flux in the plasma). A particular configuration with the inner $R_i = 0.5\,\text{m}$ and outer $R_e = 2.0\,\text{m}$ radii and the plasma height 3 m is considered. The entire plasma of such an ST would fit into the ITER-FEAT plasma cross-section. The plasma volume $V = 26\,\text{m}^3$ and the surface $S = 53.4\,\text{m}^2$ are about 30 and 12 times smaller than the corresponding plasma volume and surface of ITER-FEAT.

The value of the toroidal magnetic field $B_{tor} = 7.5\,\text{T}$ at $R = R_i$ and 3 T at the plasma geometric center is technically feasible and would be sufficient for robust plasma stabilization at $\beta \simeq 0.4$–0.45 with the pressure exceeding the OPRR level of 1 MPA. A flat parallel current density $j_\parallel$ is assumed for the current distribution together with the simplest model of the pressure distribution $dp/d\Psi = \text{const}$. In contrast to the conventional plasma, an IST with a finite current density at the edge and wall stabilization does not require pressure profile tailoring.

Such an IST configuration would have fusion power $P_{DT} = 658\,\text{MW}$ (with $P_{rad} = 36.5\,\text{MW}$ at $Z_{eff} \simeq 1$) and would require only $\overline{\tau}_E^* = 0.49\,\text{s}$ (or, with radiation subtracted, $\tau_E^* = 0.68\,\text{s}$) energy confinement time. Its total current $I_{pl} = 8.5\,\text{MA}$ should be initiated by inductive current drive, while after ignition it will be maintained and, in fact, enhanced by the bootstrap current drive.

The IST configuration has other properties consistent with the requirements for development of the FW and TC. Thus, with only 10% neutron loss in the central rod (52 MW of the power in neutrons), the average neutron load on the outer wall is $10.7\,\text{MW/m}^2$, which exceeds by an order of magnitude projections based on conventional plasma regimes.

6.2. Self-sufficiency of bootstrap current

In consideration of a stationary plasma with low edge temperature there is always a conflict between stability of free boundary MHD modes and high value of

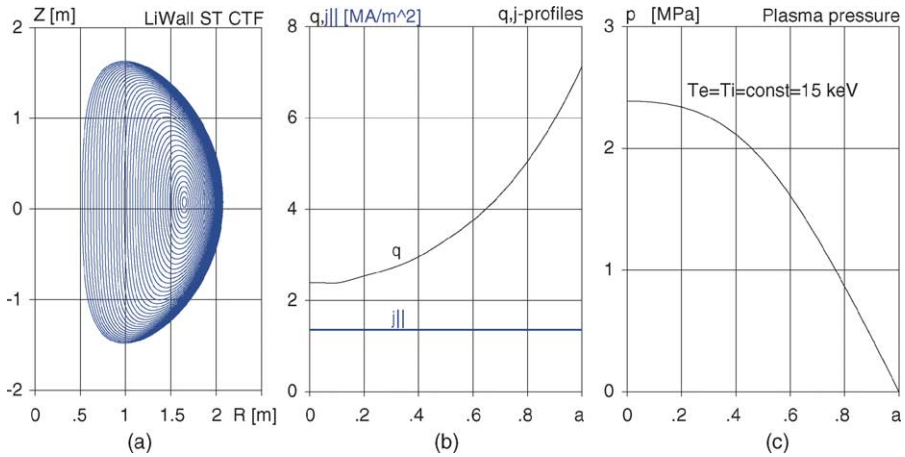

Fig. 9. (a) Stable magnetic configuration of ignited spherical tokamak with $I_{pl} = 8.5\,\text{MA}$, $\beta = 0.46$. (b) Parallel current density and q-profile. (c) Pressure profile (exceeding OPRR level).

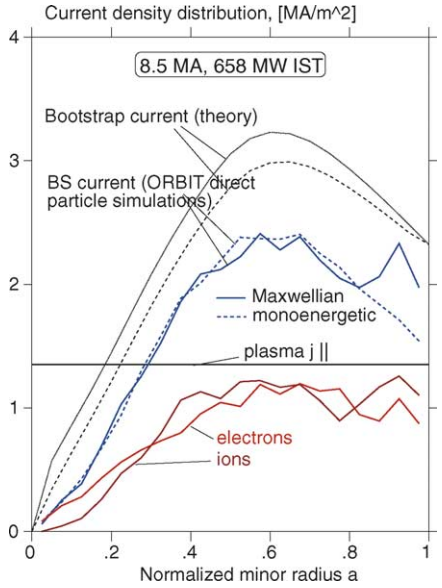

Fig. 10. Bootstrap current profile in IST configuration of Fig. 9.

the bootstrap current. For optimization it would require the so-called "profile control". In contrast, with a flat $T_{i,e} \simeq$ const. $= 15$ the LiWall stabilized IST configurations can be overdriven by bootstrap current without violating stability.

The bootstrap current calculations for the IST configuration of Fig. 9 are shown in Fig. 10. The ORBIT code (R. White) has been used for calculation of the bootstrap current based on direct particle orbit simulations. The blue curves (dashed and solid) in Fig. 10 represent the bootstrap current calculated with Maxwellian and mono-energetic particle distribution functions. The red and brown curves are contributions from ions and electrons. The standard theory, developed for conventional aspect ratio [27] gives 25% higher value than the particle simulations. The black dotted curve represents the collisionless theory model and black dashed curve results from the theory with collisions at $T = 15$ keV. (At this moment, the reason of some discrepancy between theory and particle simulation results is not yet understood.)

The solid black line in Fig. 10 represents the parallel current distribution in the configuration. Both particle orbit simulation and the theory indicate a significant value of the bootstrap current over $j_{\|}$ everywhere except in the plasma center.

Bootstrap current overdrive does not represent a problem for the IST. The IST provides a wide operational space for variations of plasma current density and pressure, even at a level exceeding OPRR requirements. In particular, a stationary configuration with almost 100% alignment of the bootstrap current with the plasma current is achievable with no deterioration of stability or the fusion power.

Fig. 11 shows an example of a configuration, with a pressure profile similar to the previous case and the

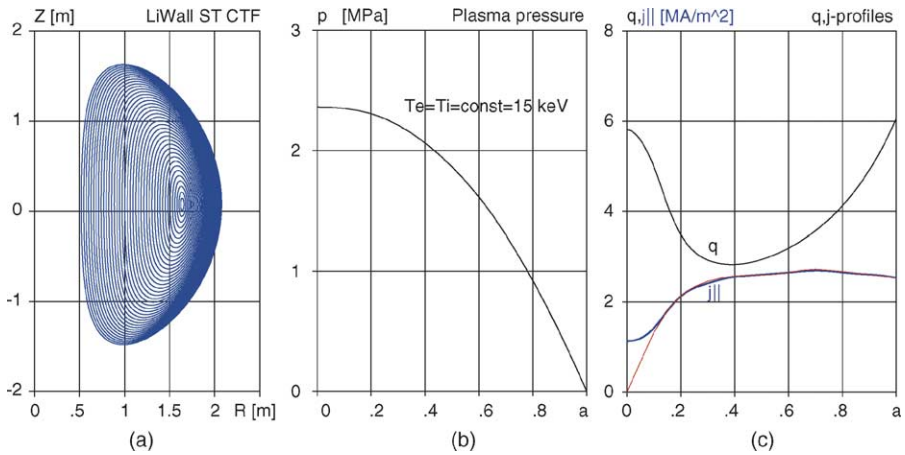

Fig. 11. (a) Stable magnetic configuration of bootstrap current maintained IST configuration with $I_{\rm pl} = 9.2$ MA, $\beta = 0.44$. (b) Parallel current density $j_{\|}$ (blue) aligned with the bootstrap current (red) and q-profile. (c) Pressure profile. For interpretation of the references to color in this figure legend, the reader is referred to the web version of this article.

current profile aligned with the bootstrap current everywhere, except for a small region near the magnetic axis. Here, the bootstrap current has been calculated using orbit particle calculations as a normalization for theory formulas. This configuration has a fusion power $P_{DT} = 649\,MW$ ($P_{rad} = 36\,MW$) and requires the same energy confinement time for ignited operation ($\overline{\tau}_E^* = 0.49\,s$, $\tau_E^* = 0.68\,s$).

Note that the center region is the most favorable for the radio-frequency current drive methods because of the reduced fraction of trapped electrons. Thus, the deficiency in the bootstrap current in the small central zone could be, if necessary, compensated by other kinds of current drive.

6.3. Magnetic well, suppression of micro-instability

An exceptional property of the IST configuration is that it has an absolute magnetic well inside the plasma. Fig. 12 shows the amplitude of the total magnetic field $|B|$, calculated along the θ =const-lines in the radial direction (θ is the poloidal angle in the cross-section). In the plot n is the toroidal wave number of the mode,

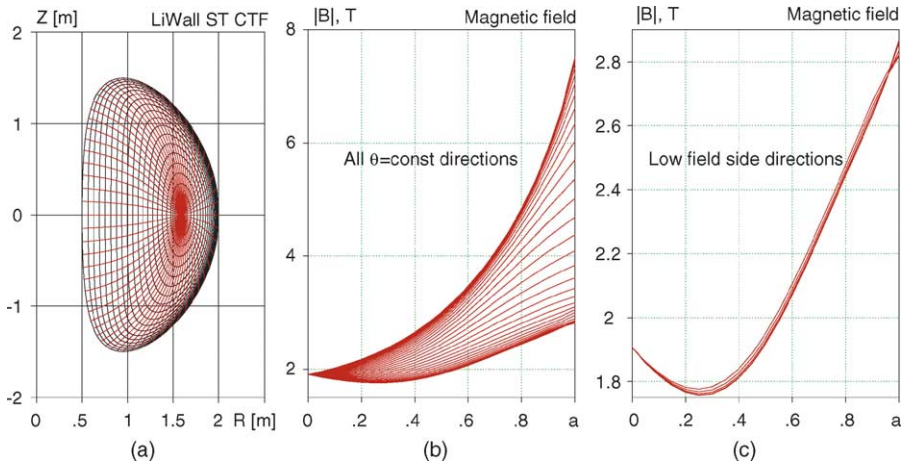

Fig. 12. (a) Stable magnetic configuration of Fig. 9 (IST with $I_{pl} = 8.5\,MA$, $\beta = 0.46$). Red lines correspond to θ = const. (b) $|B|$ as a function of a for 64 equidistant θ values. (c) $|B|$ as a function of a for 5 θ values near the outer middle plane. For interpretation of the references to color in this figure legend, the reader is referred to the web version of this article.

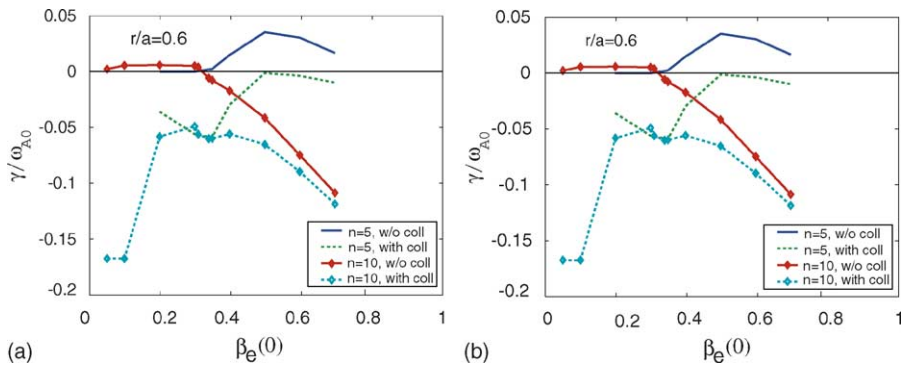

Fig. 13. (a) Growth rate of ETM at $a = 0.6$ as a function of electron $\beta_e(0)$. (b) Growth rate of $n = 5$ ETM mode (most unstable) as a function of a at $\beta_e(0) = 0.7$, corresponding to ITS parameters of Fig. 9. Solid curves corresponds neglecting collisions, dotted curves are calculated with collisions at $T = 15\,keV$.

γ, ω_{A0} are the growth rate and Alfven frequency, correspondingly.

Fig. 12c shows that an absolute minimum of $|B|$ exists inside the plasma between the magnetic axis and the outer edge. The field gradient at the outer board of IST reaches a value

$$\left.\frac{\mathrm{d}|B|}{|B|\,\mathrm{d}R}\right|_{\theta=0} \simeq 2\,\mathrm{m}^{-1}, \tag{35}$$

which is much larger than the curvature of the magnetic field lines $1/R$. In this situation, the plasma particle precession reverses its direction and puts electrons out of resonance with diamagnetic frequency. As a result, the trapped particle instabilities can be stabilized [28–31], thus, removing the residual turbulence from the D-region of low recycling plasma.

Fig. 13 shows such a stabilization of electron trapped modes (ETM) by enhanced beta in IST configuration, calculated using the HINST code [32].

Increase in β stabilizes modes as is shown in Fig. 13a. All modes with $n > 5$ become stabilized independent of the effect of collisions (stabilizing). At the full plasma pressure, even the $n = 5$ mode is completely stable at $a > 0.6$.

Thus, at high β of IST, the electron trapped modes can be stabilized by reversed particle precession. In this case, with no micro-turbulence present in the D-region of the low recycling plasma, the configuration can, potentially, approach the condition of D^3He fusion, (requiring higher plasma temperature and about 25–50 times, depending on dilution by α-particles, better confinement [33]). At the same time, our consideration of the OPRR, which requires a high power density, suggests that for power production the D^3He (or other "advanced" fuel) fusion is impractical.

7. Summary

As an approach to a fusion reactor the conventional tokamak plasma has insufficient performance. Limited by degradation of confinement at increased power and by low stable β, such a plasma can reach, at the best, only "burning" or ignition conditions. Fundamental plasma physics limitations prevent the conventional plasma from achieving the operational power reactor regime. In addition, technology aspects related to the solid wall environment (discussed elsewhere [34]), make the conventional plasma inconsistent with the high power density of the power reactor.

Another kind of plasma is required to achieve the key objectives of magnetic fusion, i.e., development of OPRR, first wall and tritium cycle. The concept, discussed in this paper, suggests the LiWall regime suitable to both OPRR and to its development path. The LiWall regime is also consistent with new technology approaches (e.g., liquid lithium walls) required for first wall development.

Ignited spherical tokamaks, or ISTs, suggested in the paper as an implementation of the LiWall concept, could be practical devices for developing elements of the power reactor, including ignition, obtaining parameters of the operational regime, designing the first wall and starting the tritium cycle technology. Basic theoretical limits for stable β and bootstrap current, being very restrictive for the conventional plasma, provide a wide parameter space for stationary ignited operation of IST with the wall-stabilized plasma and with a flattened temperature. The real question is to what extent these opportunities can be materialized.

While potentially eliminating or, at least, downgrading numerous problems related to plasma physics (ITG turbulence, sawtooth oscillations, free-boundary modes, impurities, Troyon β-limits, etc.) and to technology (localized power deposition, activation, difficulties with plasma stability control and use of FLiBe, etc.) the LiWall concept depends crucially on solving several issues. Some of them are common with the conventional plasma while others are specific to LiWalls.

The outstanding problem is the feasibility of core fueling. It determines the extent of the D-region in the outer plasma core and, thus, the degree of confinement improvement over the conventional plasma. In fact, core fueling is required anyway (e.g., for tritium fueling) even in the conventional reactor considerations. The second problem, specific for LiWalls, is electron behavior at the Li surface. Thus, any excessive secondary electron emission from the wall into the plasma would cool down the plasma electrons, thus, preventing the high temperature edge. The third problem is the helium ash pumping, which would probably require a different solution at the

stage of IST and in the reactor. LiWalls and ISTs open also an unexplored area of tokamak stability research associated with a deep core second stability regime and wall limited high temperature plasmas.

Despite the existence of a number of conceptual problems, the low recycling plasma is more advanced than the conventional one essentially in all reactor relevant aspects. Its comprehensive study would open new opportunities for both plasma physics and technology of the fusion reactor. By significantly extending the scope of plasma regimes, the high edge temperature plasma can also uniquely contribute to the fundamental physics of plasma stability and confinement.

Acknowledgments

This work was supported by United States Department of Energy contracts nos. DE-AC02-76-CHO-3073.

References

[1] R. Aymar, V. Chuyanov, M. Huguet, Y. Shimomura, Nucl. Fusion 41 (2001) 1301.
[2] A.M. Dimits, et al., Phys. Plasmas 7 (2000) 969.
[3] ITER Physics Expert Group on Confinement and Transport, ITER Physics Expert Group on Confinement Modelling and Database and ITER Physics Basis Editors, Nucl. Fusion 39 (1999) 2175.
[4] F. Troyon, et al., Plasma Phys. Contr. Fusion 26 (1984) 209.
[5] Y. Shimomura, et al., Nucl. Fusion 41 (2001) 309.
[6] F. Porcelli, D. Boucher, M.N. Rosenbluth, Plasma Phys. Contr. Fusion 38 (1996) 2163.
[7] M. Greenwald, et al., Nucl. Fusion 28 (1988) 2199.
[8] G.H. Miley, H. Towner, N. Ivich, AEC Report COO-2218-17, NE Program, Univ. of Illinois, 1974.
[9] D.L. Book, NRL Publication 177-4405, NRL, Washington, DC, 1990, p. 57.
[10] D.L. Book, NRL Publication 177-4405, NRL, Washington, 1990, p. 31.
[11] L.E. Zakharov, Phys. Rev. Lett. 90 (2003) 045001.
[12] D.K. Mansfield, et al., Nucl. Fusion 41 (2001) 1823.
[13] D.A. Ernst, et al., Nucl. Fusion 38 (1998) 13.
[14] C.M. Greenfield, et al., Plasma Phys. Contr. Fusion 44 (2002) 123.
[15] W.Dorland, M. Kotschenreuther, M.A. Beer, G.W. Hammett, in: Proceedings of the 15th International Conference on Plasma Physics and Controlled Nuclear Fusion Research, vol. 3, Seville, 1994, International Atomic Energy Agency, Vienna, 1995, p. 463.
[16] M. Kotschenreuther, W. Dorland, M.A. Beer, G.W. Hammett, Phys. Plasmas 2 (1995) 2381.
[17] V.B. Lazarev, A.G. Alekseev, A.M. Belov, S.V. Mirnov, Plasma Phys. Rep. 28 (2002) 802.
[18] V.B. Lazarev, et al., in: Proceedings of the 26th EPS Conference on Controlled Fusion and Plasma Physics, vol. 23J, Maastricht, June 14–18, ECA, Geneva, 1999, p. 845.
[19] V. Evtikhin, et al., in: Proceedings of the 18th International Conference on Plasma Physics and Controlled Nuclear Fusion Research, vol. EXP4, Sorrento, Italy, International Atomic Energy Agency, 2000, p. 21. http://www.iaea.or.at/programmes/ripc/physics/fec2000/html/fec2000.htm.
[20] V. Evtikhin, et al., Fusion Eng. Des. 56–57 (2001) 363.
[21] G.Y. Antar, et al., Fusion Eng. Des. 60 (2002) 157.
[22] R. Kaita, et al., Fusion Eng. Des. 61–62 (2002) 217.
[23] R. Majeski, et al., J. Nucl. Mater. 313–316 (2003) 625.
[24] M.V. Umansky, S.I. Krasheninnikov, B. LaBombard, J.L. Terry, Phys. Plasmas 5 (1998) 3373.
[25] M.V. Umansky, et al., Phys. Plasmas 6 (1999) 2791.
[26] D.A. Gates, Phys. Plasmas 10 (2003) 1659.
[27] S.P. Hirshman, Phys. Fluids 31 (1988) 3150.
[28] M. Rosenbluth, M.S. Sloan, Phys. Fluids 14 (1971) 1725.
[29] C. Bourdelle, et al., Phys. Plasmas 10 (2003) 2881.
[30] J.C. Adam, W.M. Tang, P.H. Rutherford, Phys. Fluids 19 (1976) 561.
[31] W.M. Tang, G. Rewoldt, L. Chen, Phys. Fluids B B29 (1986) 3715.
[32] N.N. Gorelenkov, et al., Phys. Plasmas 3 (1996) 3379.
[33] W.M. Nevins, J. Fusion Energy 17 (1998) 25.
[34] M.A. Abdou, et al., Fusion Eng. Des. 54 (2001) 181.